Thermal rectification induced by geometrical asymmetry: A two-dimensional multiparticle Lorentz gas model

Huan Wang,[1] Yu Yang,[1] Hongyuan Chen,[1] Nianbei Li,[2,*] and Lifa Zhang[1,†]

[1]*NNU-SULI Thermal Energy Research Center (NSTER) and Center for Quantum Transport and Thermal Energy Science (CQTES), School of Physics and Technology, Nanjing Normal University, Nanjing, 210023, China*

[2]*Institute of Systems Science and Department of Physics, College of Information Science and Engineering, Huaqiao University, Xiamen 361021, China*

(Received 26 March 2019; published 12 June 2019)

We propose a two-dimensional (2D) multiparticle Lorentz gas model by combining the direct simulation Monte Carlo method with the Lorentz gas model, where the normal thermal transport under Fourier's law is confirmed by length-independent thermal conductivity. For this 2D multiparticle Lorentz gas model, the thermal rectification effect is obtained with the asymmetrical setup of a trapezoidal shape, which is a purely geometric effect. Furthermore, we find a scaling behavior between the rectification ratio and the geometrical parameters of the trapezoidal shape, which is verified by numerical simulations.

DOI: 10.1103/PhysRevE.99.062111

I. INTRODUCTION

As the size of electronic devices constantly shrinks due to the fast development of nanotechnology, the manipulating of heat flow in such a scale has been attracting more and more interest [1]. The novel design of functioning thermal devices covers thermal diodes [2–5], thermal transistors [6], thermal memory [7], thermal ratchets [8,9], and thermal logic gates [10], to name a few. Among all the useful designs of thermal devices, the thermal diode is the very basic and important one with the most possible applications. In such a thermal diode, the heat flow can be rectified by switching the direction of the temperature gradient. The heat current in one specific direction can be larger than the other if the hot and cold sources at two ends are interchanged. Besides the nonlinearity, asymmetry is the other necessary condition to achieve thermal rectification [11–13]. Although the first theoretical design of a solid thermal diode contains three component materials to realize the asymmetric requirement [2], various works demonstrate that an efficient thermal diode usually consists of two different materials directly coupled together [3–5]. In addition, there are also some works realizing thermal rectification in models consisting of only one material where symmetry breaking is introduced by a mass gradient [14–17].

There are two major underlying mechanisms behind the effect of thermal rectification [1]. The first mechanism relies on the match or mismatch of the phonon spectra of the two-component materials [2–4]. At least one of the two-component materials should be strongly nonlinear yielding the temperature-tuned phonon spectrum. With a hot source in one end, the overlap of the phonon spectra in two sides will be significantly larger than that if the hot source is put to the other end, giving rise to efficient thermal rectification. The advantage of this kind of thermal diode is the theoretically predicted high rectification ratio, while the disadvantage is the lack of real materials with such a strong nonlinearity limiting its application. The experimental realization has been done for quasi-one-dimensional (1D) nanotubes while the rectification ratio is small [18]. The other mechanism utilizes the opposite temperature dependence of thermal conductivities for the two-component materials [19–23]. It is straightforward that larger heat current can be obtained if both component materials are located at high thermal conductivity conditions. The theoretically predicted rectification ratio may not be very large for this case, but the realization with real materials is much simpler. Many experimental efforts have been done in this direction to achieve a satisfactory thermal diode [24–28].

The successful fabrication of graphene and its high thermal conductivities has triggered the study of thermal properties of two-dimensional (2D) materials [29,30]. The thermal diode based on 2D materials has also been tackled with molecular dynamics (MD) simulations [31–34]. The 2D thermal diode can be designed by coupling two different 2D materials [31], by combining one 2D material and one quasi-1D material [32], or simply by adding asymmetric defects and disorders on one 2D material [33]. It is well known that transport properties can be influenced by the geometrical features [35–38]. However, there are few studies of the purely geometric shape effect on 2D thermal rectification [33,34]. The geometric shape-induced thermal rectification has been investigated for triangle graphene nanoribbons (GNRs), while the underlying reason has been attributed to the intrinsic angle-dependent thermal conductivity for 2D GNRs [33]. Therefore, it is still unclear whether a purely geometric shape effect can induce 2D thermal rectification or not. In this work, we will study the thermal rectification effect of a 2D Lorentz gas model which is isotropic for heat conduction. It will be found that the rectification of heat flow can be induced by a purely geometric shape effect, which is a unique property of 2D materials.

*nbli@hqu.edu.cn
†phyzlf@njnu.edu.cn

This paper is organized as follows. In Sec. II the detailed description of the 2D Lorentz gas model will be introduced. In Sec. III the thermal rectification effect and its universal scaling behavior with a geometric parameter will be presented and discussed. Finally, the conclusion will be summarized in Sec. IV.

II. 2D LORENTZ GAS MODEL

The Lorentz gas model, which was introduced in 1905 as a model for the motion of an electron in a metallic body [39], has been studied extensively in the area of mathematics and physics [40,41]. Generally, the Lorentz model consists of particles moving in an array of fixed scatterers, which are placed either periodically or randomly, and the particles are either reflected specularly off the scatterers (hard core model) or pushed away due to the potential (soft core model).

This normal Lorentz gas model is effectively a quasi-1D model by simulating particle's behavior from the collisions between the single particle and the added media in the space [42–45]. Therefore this model has some limitations when showing complex physical processes. If the simulation of multiparticle physical collisions is directly carried out as in MD method, the computational complexity is too high and the simulation scales in both time and space are very limited. However, the direct simulation Monte Carlo method (DSMC) method [46–48] can effectively solve the above mentioned difficulties. It was proposed by Bird in the 1960s that the DSMC method is a numerical method for modeling rarefied gas flows, in which the mean-free path of a molecule is of the same order (or greater) than a representative physical length scale (i.e., the Knudsen number K_n is greater than 1). By combining the DSMC method and the normal Lorentz gas model, we here propose a multiparticle 2D Lorentz gas model.

The idea of the DSMC method is to decouple the translation and collision of particles. The area will be separated into several spaces, and then only the collisions among the particles in the same space will be considered. By doing so, the K-means clustering algorithm [49] is applied to randomly select K objects as the initial clustering center. Then we calculate the distance between each particle and each clustering center to assign each particle to its nearest cluster center. A cluster consists of a clustering center and the particles assigned to this center. Once all the objects have been assigned, the cluster center for each cluster is recalculated based on the existing particles in the cluster. This process will be repeated until a certain termination condition is satisfied. The termination condition may be that no (or a minimum number of) particles are reassigned to different clusters, or none (or a minimum number) of the cluster centers will change again, or the sum of squared errors has been minimized. The clustering center mentioned in this K-means algorithm is the divided space in our model.

The way to decide the collisions relies on probability consideration instead of comparing the distance between the particles with their radius. Therefore, by combining the DSMC method with the Lorentz gas model, we can easily realize the multiparticle Lorentz gas model in a 2D trapezoidal space. The mean-free path here for the particles is estimated as 0.035 in the dimensionless unit, which is much smaller than the geometric size we will use.

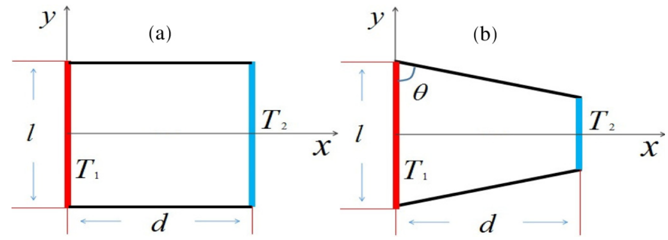

FIG. 1. (a) The 2D Lorentz gas model with a symmetric rectangular shape. T_1 is the temperature of the left heat reservoir, and T_2 is the temperature of the right heat reservoir. l and d are the width and length of this rectangular space, respectively. (b) The 2D Lorentz gas model with an asymmetric trapezoidal shape. Parameter θ is the angle between the top boundary and the left boundary.

The 2D rectangular setup of the Lorentz gas model can be seen in Fig. 1(a). The length and width of the rectangular space are denoted as d and l, respectively. The temperature sources T_1 and T_2 are put in contact with the two end lines with $x = 0$ and $x = d$. The top and bottom of the space is set to be a thermal insulator, so the particles just make a mirror reflect when they collide with these two sides. When it comes to the temperature sources (left and right sides), first the particle is absorbed by the heat reservoir, and then the heat reservoir will release a particle in return, whose velocity distribution is defined by the following equation [42]:

$$P(v_x) = \frac{m}{kT} v_x e^{-\frac{mv_x^2}{2kT}}, \tag{1}$$

$$P(v_y) = \sqrt{\frac{m}{2\pi kT}} e^{-\frac{mv_y^2}{2kT}}. \tag{2}$$

In order to calculate the heat flux, it is noticed that as the system has reached a stationary state after a long enough relaxed time, the energy released by the high-temperature source will be equal to the energy absorbed by the low-temperature source. Therefore, we need to collect only the information about the energy of the absorbed and released particle of one temperature source over a period of time, and then the heat flux of the system can be numerically calculated. The temperature can be calculated for every particle as the position and kinetic energy of each particle at any moment can be obtained during the simulation. With the information on the heat flux and temperature distribution, the thermal conductivity κ of the system can be obtained:

$$I = \frac{dE}{dt}, E = E_{\text{released}} - E_{\text{absorbed}}, \tag{3}$$

$$T(x) = \frac{E(x)}{k_B}, \tag{4}$$

$$I = -\kappa \frac{dT}{dx}. \tag{5}$$

For 2D nonlinear lattice systems, the thermal conductivity κ is predicted to diverge in a logarithmic way with the system size [50]. This logarithmic divergence of thermal conductivity has been verified by experiments on graphene [51]. The energy carriers in 2D lattice systems are collective motions

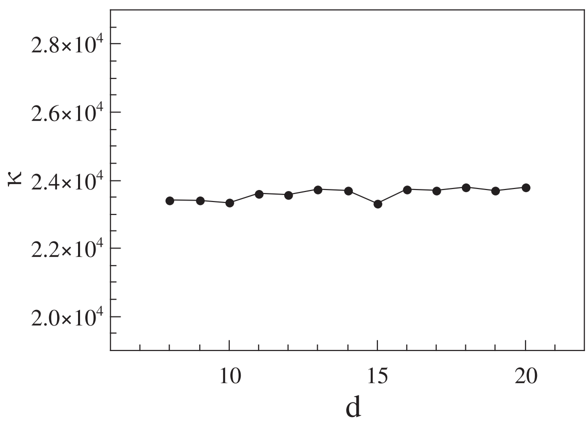

FIG. 2. The length-dependent thermal conductivity κ calculated for a rectangular 2D Lorentz gas model. The width l of the rectangular space is set as a constant value $l = 10$. The hot temperature source is fixed as $T_1 = 400$ K, and the cold temperature source is fixed as $T_2 = 200$ K. The length of the rectangular space d changes from 8 to 20, and it can be seen that thermal conductivity κ does not vary with the system length indicating normal heat conduction behavior. In each calculation, thousands of particles are simulated within the 2D rectangular space.

of virtual phonons, and long-wave length phonons can induce the anomalous heat conduction found in low dimensions, including 1D and 2D lattice systems [50]. In our proposed 2D Lorentz gas model, the energy carriers are the real moving particles.

To check the heat conduction in our 2D Lorentz gas model, we calculate the thermal conductivity κ in a rectangular space depicted in Fig. 1. The width l in dimensionless units of this rectangular space is fixed at $l = 10$, and the length d is varied from $d = 8$ to $d = 20$. In Fig. 2 the thermal conductivities κ of this 2D Lorentz gas model in a rectangular shape with hot and cold temperature sources fixed at $T_1 = 400$ K and $T_2 = 200$ K are plotted. It can be seen that as the system length d increases, the thermal conductivity κ remains a constant value. These results indicate that our 2D Lorentz gas model follows Fourier's heat conduction law and possesses normal heat conduction behavior. The reason for normal heat conduction in the 2D Lorentz gas model is that the mean-free path of particles is very much limited due to collisions, in contrast to the diverging mean-free path of long-wave length phonons in low-dimensional lattice systems.

III. THERMAL RECTIFICATION INDUCED BY A PURELY GEOMETRIC SHAPE EFFECT

In order to have thermal rectification, two necessary conditions are required, which are nonlinearity and asymmetry [1]. The previous design of a thermal diode usually couples two different materials to achieve asymmetry. However, for a 2D system, the natural choice of asymmetric condition is simply realized by changing the rectangular space into a trapezoidal space, as plotted in Fig. 1(b).

In the 2D asymmetric trapezoidal Lorentz gas model, the width l of the left end remains unchanged, while the width of the right end can be adjusted from l to 0. The new parameter θ is the angle between left and top boundaries of the trapezoidal space, and the value of $\tan\theta$ is tuned from infinity to $\tan\theta = \frac{d}{l/2}$ as the right width is changed from l to 0. The cases of $\tan\theta = \infty$ and $\tan\theta = \frac{d}{l/2}$ denote the limiting cases of rectangular and triangular spaces, respectively.

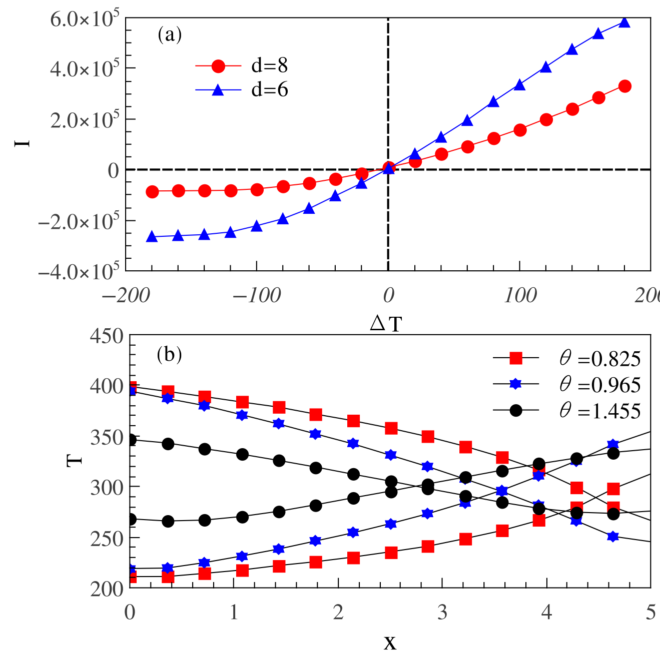

FIG. 3. (a) Heat flux I as the function of temperature difference ΔT for the 2D Lorentz gas model with asymmetric trapezoidal shape. The average temperature T_0 is fixed at $T_0 = 200$ K. The left and right temperature sources T_1 and T_2 are set as $T_1 = T_0 + \Delta T$ and $T_2 = T_0 - \Delta T$, respectively. The left width l is chosen as $l = 10$, and the angle θ is fixed at $\theta = \frac{\pi}{3}$. For two different cases with length $d = 6$ and 8, asymmetric I-ΔT dependence is observed, indicating a thermal rectification effect. (b) Temperature distributions $T(x)$ with reversing temperature sources for the 2D Lorentz gas model. The average temperature and temperature difference are fixed at $T_0 = 300$ K and $\Delta T = 100$ K. The left width and length are chosen as $l = 10$ and $d = 5$. The asymmetric temperature distributions can be obtained for three different angles $\theta = 1.455,\ 0.965$, and 0.825. It is also clear that as the the angle θ gets smaller, the asymmetry of the temperature distributions in the forward and backward directions is more obvious.

The thermal rectification ratio R is defined as [3]

$$R = \left|\frac{I_+ - I_-}{I_+ + I_-}\right|, \tag{6}$$

where I_+ is the absolute value of the forward heat flow when $T_1 > T_2$ and I_- is the absolute value of the backward heat flow when $T_2 > T_1$. With such a definition, $R = 0$ describes the situation with no thermal rectification, and $R = 1$ denotes the situation with a perfect thermal diode effect.

In Fig. 3(a) the heat flux I as the function of ΔT for a trapezoidal 2D Lorentz gas model is plotted. The left and right temperatures T_1 and T_2 are set as $T_1 = T_0 + \Delta T$ and $T_2 = T_0 - \Delta T$ with $T_0 = 200$ K the average temperature. The left width l and angle θ are fixed at $l = 10$ and $\theta = \pi/3$. Two different cases of system length $d = 6$ and 8 are considered,

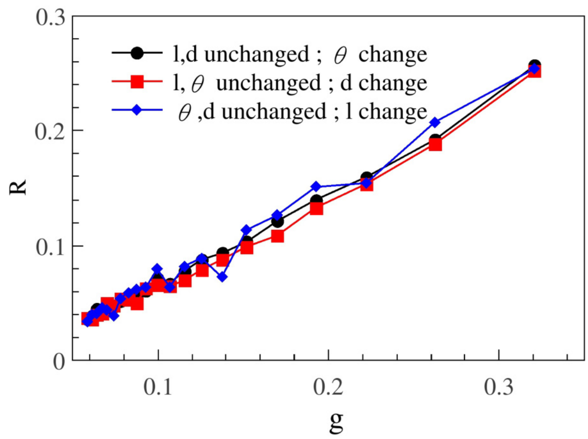

FIG. 4. The rectification ratio R as the function of the reduced geometric parameter $g = d/l \tan\theta$. The average temperature T_0 and temperature difference ΔT are fixed at $T_0 = 350$ K and $\Delta T = 250$ K, respectively. The data with black circles represent the parameter setup of $(l = 10, d = 5)$ with θ varying from $\pi/2$ to 0.890. The data with red squares denote the parameter setup of $(l = 10,\ \theta = \pi/4)$ with d changing from 0 to 5. The data with blue diamonds depict the parameter setup of $(d = 5,\ \theta = \pi/4)$ with l ranging from 50 to 10. The rectification ratio R exhibits a universal behavior with the reduced geometric parameter g.

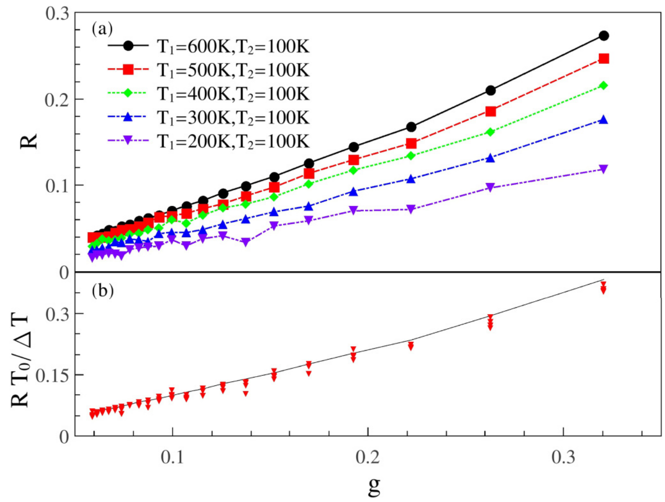

FIG. 5. (a) The rectification ratio R as the function of g for different temperature pairs (T_1, T_2). The cold temperature is fixed at $T_2 = 100$ K, and the hot temperature source takes values of $T_1 = 200, 300, 400, 500, 600$ K. (b) The modified ratio of $RT_0/\Delta T$ as the function of g for different temperature pairs. All the curves collapse into one single curve showing a universal scaling as the function of $\Delta T/T_0$.

and the resulting I-ΔT curves are asymmetric, which is a clear sign of the thermal rectification phenomenon.

To identify rectification of the heat flux, it is also useful to check the temperature distributions $T(x)$ in the forward and backward directions. In Fig. 3(b) the forward and backward temperature distributions $T(x)$ are plotted for three different angles $\theta = 1.455$, 0.965, and 0.825. The other parameters are kept the same as $l = 10, d = 5, T_0 = 300$ K, and $\Delta T = 100$ K. It can be seen that the temperature distributions $T(x)$ are not symmetric for the forward and backward directions. In particular, as the angle θ decreases, the temperature distributions $T(x)$ are more asymmetric. Both the asymmetric I-ΔT curves and temperature distributions $T(x)$ in the forward and backward directions clearly demonstrate that the thermal rectification can be induced purely by a geometric shape effect in the 2D Lorentz gas model. This is a unique property of 2D homogeneous systems.

The degree of the asymmetry of the trapezoidal space determines the final rectification of heat flux. As can be seen in Fig. 1(b), there are three parameters controlling the asymmetry of the systems: the left width l, the angle θ, and the length d. In principle, the rectification ratio R can be tuned by adjusting each of these three geometric parameters. The most interesting thing is that the rectification effect shows a universal dependence as the function of a reduced geometric parameter g, which is defined as

$$g = \frac{d}{l\tan\theta}, \tag{7}$$

which takes values between [0, 1/2] as θ changes, with $g = 0$ and $g = 1/2$ representing the rectangular and triangular space, respectively.

In Fig. 4 we plot the thermal rectification ratio R as the function of the reduced geometric parameter g. The average temperature is set as $T_0 = 350$ K and the temperature difference is fixed at $\Delta T = 250$ K. The reduced geometric parameter g is a combination of three parameters (d, l, θ). We consider three different approaches to adjust the reduced geometric parameter g. In the first approach, the parameters of left width l and length d are fixed at $(l = 10,\ d = 5)$. The only left parameter of the angle θ is varied from 0 to $\pi/4$ to adjust g from 0.06 to 0.32 (the black circles in Fig. 4). In the second approach, the parameters of the left width l and angle θ are fixed at $(l = 10,\ \theta = \pi/4)$. The only left parameter of the length d is changed from 0 to 5 tuning the parameter g from 0.06 to 0.32 (the red squares in Fig. 4). In the third approach, the parameters of length d and angle θ are fixed at $(d = 5, \theta = \pi/4)$. The only left parameter of the left width l is adjusted from 50 to 10, yielding the parameter g from 0.06 to 0.32 (the blue diamonds in Fig. 4). It is striking to find that all three curves collapse into each other, exhibiting a universal dependence between the rectification ratio R and the reduced geometric parameter g. As can be seen in Fig. 4, the thermal rectification ratio R depends universally on the reduced geometric parameter g almost in a linear way:

$$R \propto g. \tag{8}$$

If we introduce parameter r as the right width of the trapezoidal space in Fig. 1(b), it can be noticed that $\tan\theta = \frac{d}{(l-r)/2}$. The reduced geometric parameter g can be reexpressed as $g = d/l\tan\theta = \frac{1}{2}(1 - r/l)$. Although we have three geometric parameters d, l, and $\tan\theta$ to control, the reduced geometric parameter g has only two independent geometric parameters, l and r. Actually the asymmetry of the trapezoidal space is induced by the difference between left and right width of l and r. For the rectangular case, the left and right width l and r are equal. As a result, the reduced geometric parameter vanishes as $g = 0$, and there is no rectification effect as we

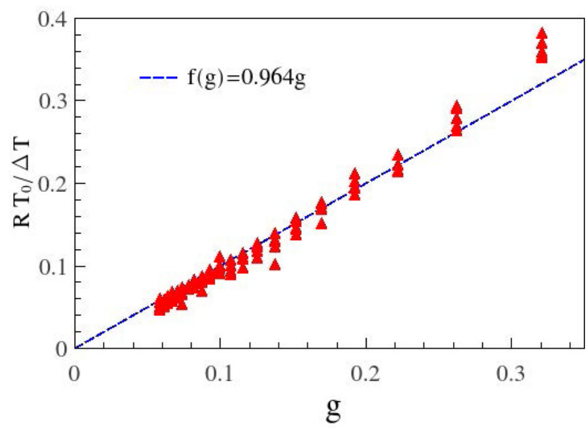

FIG. 6. The normalized rectification ratio $RT_0/\Delta T$ as the function of geometric parameter g with all the data used in previous figures. The universal scaling relation of Eq. (10) is verified.

expected. The universal dependence of $R \propto g$ reveals that the rectification effect is only a function of the asymmetric ratio r/l between the left and right width of the trapezoidal space.

We do not have data for parameter g close to 0.5, which is the triangular limit. The reason is that in this regime the numerical result is not credible due to large error. This is because when the width of the right heat reservoir is very small near the triangular limit, the overall energy flow becomes very small and the stochastic error is very large.

Besides the geometric parameters of (d, l, θ), the thermal rectification also depends on the pair of temperature sources T_1 and T_2. In Fig. 5(a) the rectification ratio R as the function of g is calculated for many different temperature pairs of (T_1, T_2). Interestingly enough, the rectification ratio R also exhibits a universal scaling with the temperature pairs as

$$R \propto \frac{T_1 - T_2}{T_1 + T_2} = \frac{\Delta T}{T_0}. \tag{9}$$

This universal scaling behavior can be clearly seen in Fig. 5(b) if we replot the rectification ratio R normalized by $\Delta T/T_0$ as the function of g. Again, all the curves collapse into one single almost linear curve implying a universal scaling between rectification ratio R and $\Delta T/T_0$.

In general, the rectification effect is enhanced as the asymmetric temperature field of ΔT increases. The extra-temperature dependence of $R \propto 1/T_0$ might come from the fact that the average velocity $\bar{v}$ of particle is proportional to the square of the average temperature as $\bar{v} \propto \sqrt{T_0}$. The influence of the asymmetry of the trapezoidal space will be smeared by the increase of the particle mean velocity $\bar{v}$. As a result, the rectification effect will be decreased as the average temperature T_0 increases in a qualitative way.

Combining the geometric and temperature effects, the rectification ratio R can be expressed as the following scaling relation:

$$R \propto g\frac{\Delta T}{T_0}, \tag{10}$$

where $g = d/l \tan\theta$ is the reduced geometric parameter, $T_0 = (T_1 + T_2)/2$ is the average temperature, and $\Delta T = (T_1 - T_2)/2$ is the half temperature difference.

To verify the universal scaling relation of Eq. (10), in Fig. 6 we plot the normalized rectification ratio $RT_0/\Delta T$ as the function of geometric parameter g with all the data we used in previous figures. Here we use coefficient of determination R^2 to measure the goodness of the fit and $R^2 = 0.961$. A clear linear dependence between $RT_0/\Delta T$ and g can be observed. Therefore, the universal scaling of Eq. (10) for a 2D Lorentz gas model with trapezoidal shape is verified with detailed numerical simulations.

IV. CONCLUSION

In summary, we have proposed a 2D Lorentz gas model to investigate the thermal rectification effect induced by a purely geometric shape asymmetry. The 2D Lorentz gas model shows normal heat conduction behavior without size effect. If we change the rectangular space into a trapezoidal space which is asymmetric, the phenomenon of thermal rectification can be obtained. Contrary to the thermal rectification found in a 2D graphene system [33], the 2D Lorentz gas model has no intrinsic angle-dependent heat conduction. The rectification of heat flow in the 2D Lorentz gas model is therefore induced by a purely geometric shape effect. In particular, we find the thermal rectification behavior in the 2D Lorentz gas model exhibits a universal relation with the geometric parameters and source temperatures. This universal relation is well verified by our numerical results.

ACKNOWLEDGMENTS

We acknowledge support from NSFC (Grants No. 11890703, No. 11775158, and No. 11574154), from the Science and Technology Commission of Shanghai Municipality with Grant No. 17ZR1432600, and from the Scientific Research Funds of Huaqiao University.

[1] N. Li, J. Ren, L. Wang, G. Zhang, P. Hanggi, and B. Li, Rev. Mod. Phys. **84**, 1045 (2012).

[2] M. Terraneo, M. Peyrard, and G. Casati, Phys. Rev. Lett. **88**, 094302 (2002).

[3] B. Li, L. Wang, and G. Casati, Phys. Rev. Lett. **93**, 184301 (2004).

[4] B. Li, J. H. Lan, and L. Wang, Phys. Rev. Lett. **95**, 104302 (2005).

[5] B. Hu, L. Yang, and Y. Zhang, Phys. Rev. Lett. **97**, 124302 (2006).

[6] B. Li, L. Wang, and G. Casati, Appl. Phys. Lett. **88**, 143501 (2006).

[7] L. Wang and B. Li, Phys. Rev. Lett. **101**, 267203 (2008).

[8] N. Li, P. Hanggi, and B. Li, Europhys. Lett. **84**, 40009 (2008).

[9] N. Li, F. Zhan, P. Hanggi, and B. Li, Phys. Rev. E **80**, 011125 (2009).

[10] L. Wang and B. Li, Phys. Rev. Lett. **99**, 177208 (2007).

[11] L. Zhang, J.-S. Wang, and B. Li, Phys. Rev. B **81**, 100301(R) (2010).

[12] L. Zhang, J.-T. Lu, J.-S. Wang, and B. Li, J. Phys.: Condens. Matter **25**, 445801 (2013).
[13] L. Zhang, J. Thingna, D. He, J.-S. Wang, and B. Li, Europhysics. Lett. **103**, 64002 (2013).
[14] N. Yang, N. Li, L. Wang, and B. Li, Phys. Rev. B **76**, 020301(R) (2007).
[15] R. Dettori, C. Melis, R. Rurali, and L. Colombo, J. Appl. Phys. **119**, 215102 (2016).
[16] E. Pereira, Phys. Rev. E **82**, 040101(R) (2010).
[17] J. Wang, E. Pereira, and G. Casati, Phys. Rev. E **86**, 010101(R) (2012).
[18] C. W. Chang *et al.*, Science **314**, 1121 (2006).
[19] C. Dames, J. Heat Transfer **131**, 061301 (2009).
[20] D. B. Go and M. Sen, J. Heat Transfer **132**, 124502 (2010).
[21] T. Shih, Z. Gao, Z. Guo, H. Merlitz, P. Pagni, and Z. Chen, Sci. Rep. **5**, 12677 (2015).
[22] A. Arora, T. Hori, T. Shiga, and J. Shiomi, Phys. Rev. B **96**, 165419 (2017).
[23] Y. Yang, H. Chen, H. Wang, N. Li, and L. Zhang, Phys. Rev. E **98**, 042131 (2018).
[24] W. Kobayashi, Y. Teraoka, and I. Terasaki, Appl. Phys. Lett. **95**, 171905 (2009).
[25] D. Sawaki, W. Kobayashi, Y. Moritomo, and I. Terasaki, Appl. Phys. Lett. **98**, 081915 (2011).
[26] T. Takeuchi, H. Goto, R. Nakayama, Y. Terazawa, K. Ogawa, A. Yamamoto, T. Itoh, and M. Mikami, J. Appl. Phys. **111**, 093517 (2012).
[27] S. Tamura and K. Ogawa, Solid State Commun. **152**, 1906 (2012).
[28] R. Nakayama and T. Takeuchi, J. Electron. Mater. **44**, 356 (2014).
[29] K. S. Novoselov, A. K. Geim, S. V. Morozov, D. Jiang, Y. Zhang, S. V. Dubonos, I. V. Grigorieva, and A. A. Firsov, Science **306**, 666 (2004).
[30] A. A. Balandin, S. Ghosh, W. Bao, I. Calizo, D. Teweldebrhan, F. Miao, and C. N. Lau, Nano Lett. **8**, 902 (2008).
[31] A. Rajabpour, S. M. Vaez Allaei, and F. Kowsary, Appl. Phys. Lett. **99**, 051917 (2011).
[32] X. Yang, D. Xu, and B. Cao, ACS Appl. Mater. Interfaces **9**, 24078 (2017).
[33] J. Hu, X. Ruan, and Y. P. Chen, Nano Lett. **9**, 2730 (2009).
[34] N. Yang, G. Zhang, and B. Li, Appl. Phys. Lett. **95**, 033107 (2009).
[35] P. Hanggi and F. Marchesoni, Rev. Mod. Phys. **81**, 387 (2009).
[36] P. Burada, P. Hanggi, F. Marchesoni, G. Schmid, and P. Talkner, Chem. Phys. Chem. **10**, 45 (2009).
[37] X. Yang, C. Liu, Y. Li, F. Marchesoni, P. Hanggi, and H. Zhang, Proc. Natl. Acad. Sci. USA **114**, 9564 (2017).
[38] T. Mithun, C. Danieli, Y. Kati, and S. Flach, Phys. Rev. Lett. **122**, 054102 (2019).
[39] H. A. Lorentz, Proc. K. Ned. Akad. Wet. **7**, 438 (1905).
[40] C. Dettmann, Commun. Theor. Phys. **62**, 521 (2014).
[41] H. Chen, H. Wang, Y. Yang, N. Li, and L. Zhang, Phys. Rev. E **98**, 032131 (2018).
[42] D. Alonso, R. Artuso, G. Casati, and I. Guarneri, Phys. Rev. Lett. **82**, 1859 (1999).
[43] G. Casati, C. Mejia-Monasterio, and T. Prosen, Phys. Rev. Lett. **98**, 104302 (2007).
[44] H. Larralde, F. Leyvraz, and C. Mejía-Monasterio, J. Stat. Phys. **113**, 197 (2003).
[45] B. Li, G. Casati, and J. Wang, Phys. Rev. E **67**, 021204 (2003).
[46] F. J. Alexander and A. L. Garcia, Comput. Phys. **11**, 588 (1997).
[47] G. A. Bird, *Molecular Gas Dynamics* (Oxford University Press, Oxford, 1976).
[48] G. A. Bird, Phys. Fluids **13**, 2676 (1970).
[49] J. A. Hartigan and M. A. Wong, Appl. Stat. **28**, 100 (1979).
[50] S. Lepri, R. Livi, and A. Politi, Phys. Rep. **377**, 1 (2003).
[51] X. Xu, L. F. C. Pereira, Y. Wang, J. Wu, K. Zhang, X. Zhao, S. Bae, C. T. Bui, R. Xie, J. T. L. Thong, B. H. Hong, K. P. Loh, D. Donadio, B. Li, and B. Ozyilmaz, Nat. Commun. **5**, 3689 (2014).